Published in final edited form as:
Immunity. 2013 December 12; 39(6): 1108–1120. doi:10.1016/j.immuni.2013.11.009.

Salmonella Typhimurium Impedes Innate Immunity with a Mast Cell-Suppressing Tyrosine Phosphatase SptP

Hae Woong Choi[1], **Rhea Brooking**[1], **Subham Neupane**[6], **Chul-Jin Lee**[4], **Edward A. Miao**[8,9], **Herman F. Staats**[1,2,5], and **Soman N. Abraham**[1,2,3,7]

[1]Department of Pathology, Duke University Medical Center, Durham, NC 27710, USA

[2]Department of Immunology, Duke University Medical Center, Durham, NC 27710, USA

[3]Department of Molecular Genetics and Microbiology, Duke University Medical Center, Durham, NC 27710, USA

[4]Department of Biochemistry, Duke University Medical Center, Durham, NC 27710, USA

[5]Duke Human Vaccine Institute, Durham, NC 27710, USA

[6]Undergraduate Program in Biology, Duke University Medical Center, Durham, NC 27710, USA

[7]Program in Emerging Infectious Diseases, Duke-National University of Singapore, Singapore 169857, Singapore

[8]Department of Microbiology and Immunology, University of North Carolina at Chapel Hill, Chapel Hill, NC 27599, USA

[9]Lineberger Comprehensive Cancer Center, University of North Carolina at Chapel Hill, Chapel Hill, NC 27599, USA

Summary

The virulence of *Salmonella* is linked to its invasive capacity and suppression of adaptive immunity. This does not explain, however, the rapid dissemination of the pathogen after breaching the gut. Here we showed that early in infection, *S.* Typhimurium suppressed degranulation of local mast cells (MCs), resulting in limited neutrophil recruitment and restricted outflow of vascular contents into infection sites, thus facilitating bacterial spread. MC suppression was mediated by the *Salmonella* phosphatase (SptP), which shares structural homology with *Yersinia* YopH. SptP functioned by dephosphorylating the vesicle fusion protein N-ethylmalemide-sensitive factor (NSF) and by blocking phosphorylation of Syk. Without SptP, orally challenged *S.* Typhimurium failed to suppress MC degranulation and exhibited limited colonization of the mesenteric lymph nodes. Administration of SptP to sites of *Escherichia coli* infection markedly enhanced its

Correspondence and requests for materials should be addressed to: Soman N. Abraham, Ph.D., Department of Pathology, Duke University Medical Center, Box 3712, Durham, NC 27710, Phone: 919-684-3630, Fax: 919-684-2021, soman.abraham@duke.edu.

virulence. Thus, SptP-mediated inactivation of local MCs is a powerful mechanism utilized by *S.* Typhimurium to impede early innate immunity.

Introduction

The bacterial pathogen *Salmonella enterica* serovar Typhimurium (*S.* Typhimurium) is a leading cause of food-related deaths, particularly among immunocompromised individuals (Mead et al., 1999; Santos et al., 2009). *S.* Typhimurium virulence has been associated with the ability to evade and suppress the host immune system. Some of the earliest studies investigating the pathogenesis of *S.* Typhimurium highlighted its remarkable capacity to invade and persist intracellularly within gut epithelial cells and neighboring macrophages (Haraga et al., 2008), where it can replicate while avoiding immune cells and antimicrobial agents. Invasion and intracellular persistence are mediated by a variety of effector proteins encoded in *S.* Typhimurium pathogenicity islands 1 and 2 (SPI-1 and SPI-2); the majority of these are exported out of the bacterial cell by the well-characterized type III secretion system (T3SS) (Galan, 2001). One such effector is SptP, an effector protein that reverses cytoskeletal changes associated with *S.* Typhimurium entry into host cells to a pre-invasion state (Fu and Galan, 1999).

More recently, *S.* Typhimurium has been found to directly suppress host adaptive immune responses by impeding the actions of specific immune cells; for example, *S.* Typhimurium induces antigen-presenting cells to adopt distinct migratory paths (Cheminay et al., 2005; Hornef et al., 2002; McLaughlin et al., 2009) and restricts T cell proliferation and activation to limited regions of the body following infection (van der Velden et al., 2005; van der Velden et al., 2008). Other studies have pointed to a more global mechanism for the suppression of adaptive immune responses that involves targeting the draining lymph node, which is the epicenter of the adaptive immune response (St John and Abraham, 2009). *S.* Typhimurium has been shown to target and disrupt the architecture of lymph nodes by altering homeostatic chemokine gradients, resulting in aberrant immune cell trafficking and an ineffective memory response to the pathogen.

While *S.* Typhimurium is able to profoundly modulate specific immune responses to primary and therefore subsequent infections, there is also evidence that this pathogen avoids or actively suppresses the more immediate and non-specific host innate immune response. For example, *S.* Typhimurium avoids recognition by Pattern Recognition Receptors (PRRs) such as toll-like receptor-4 (TLR4) (Gunn et al., 2000; Guo et al., 1997) by selectively modifying its lipopolyssacharide (LPS) structure. However, this does not explain the ability of *S.* Typhimurium to rapidly proliferate, as other bacterial components such as flagella are readily recognized by the host PRR repertoire. The lack of an adequate innate immune response to control *S.* Typhimurium growth and spread suggests a more profound bacteria-mediated mechanism to delay or completely suppress non-specific host responses.

An important component of the innate immune response to bacterial pathogens is the mast cell (MC), a morphologically distinct type of immune cell with specialized secretory functions that is preferentially located in close proximity to the epithelium of the gastrointestinal tract and other mucosal surfaces. Given their strategic location at potential

sites of pathogen entry, MCs are among the first immune cells to perceive and react to microbial penetration of the epithelial barrier (Abraham and St John, 2010; Marshall, 2004). There is now a broad consensus that MCs are pivotal in initiating early innate immune responses to invading pathogens. Studies investigating Gram-positive and Gram-negative bacteria as well as viruses and fungi (St John and Abraham, 2013; Urb and Sheppard, 2012) have revealed that MCs promote the early clearance of pathogens. MCs possess a large repertoire of receptors that recognize and respond to various microbial components. The MC response to microbial challenge is typically biphasic. First, rapid degranulation facilitates the release of pre-formed inflammatory mediators, including tumor necrosis factor (TNF), proteases, and histamine, that initiate the early recruitment of immune cells to sites of infection (St John and Abraham, 2013). This initial response is followed by *de novo* synthesis and secretion of various immune mediators several hours later. This biphasic response permits MCs not only to initiate but to sustain critical immune responses for prolonged periods of time. Because MCs are found in close proximity to the vasculature, many MC-derived mediators readily traffic into the bloodstream, initiate blood vessel dilation, and promote the extravasation of various immune cells (Dawicki and Marshall, 2007; Suto et al., 2006). MC TNF has been implicated in the early recruitment of neutrophils to sites of *E. coli* infection and other enteric bacterial pathogens (Abraham and St John, 2010; Malaviya et al., 1996; Urb and Sheppard, 2012). In the absence of MC-derived TNF-mediated neutrophil influx, infected mice readily succumb to infections in contrast to wild-type (WT) controls (Chatterjea et al., 2005; Piliponsky et al., 2010). In addition, MCs have also been implicated in the early recruitment of natural killer (NK) and NKT cells to sites of dengue virus infection, resulting in prompt viral clearance from WT mice (St John et al., 2011), although the specific MC mediator responsible for this clearance has yet to be identified. Cumulatively, there is a large body of evidence pointing to a broad role for MCs in promoting early pathogen clearance via immune cell recruitment to sites of infection. However, to date, *S.* Typhimurium has proven to be an exception to this paradigm. Although some studies have indicated that MCs appear to contribute to *S.* Typhimurium clearance, the adoptive transfer of cultured MCs into MC-deficient mice do not significantly alter *S.* Typhimurium infection (Chatterjea et al., 2005). Furthermore, the presence of MCs during severe *S.* Typhimurium infection even appear harmful (Piliponsky et al., 2010).

Given the inconclusive role of MCs during *S.* Typhimurium infection, here we sought to more closely examine interactions between MCs and *S.* Typhimurium *in vitro* and *in vivo*. We discovered that *S.* Typhimurium possessed a remarkable capacity to inhibit the ability of MCs to mount a degranulation response to powerful stimuli such as ionomycin and IgE-mediated antigen recognition and that this inhibition was attributable to SptP, a protein tyrosine phosphatase secreted by *S.* Typhimurium T3SS. Interestingly, SptP is structurally analogous to several tyrosine phosphatases present in MCs as well as mediators found in other pathogens, such as YopH of *Yersinia pestis*. We determined that SptP appeared to dephosphorylate at least two proteins that are critical for MC degranulation. Our studies reveal the distinct ability of *S.* Typhimurium to inactivate a key modulator of host innate immunity and thereby facilitate stealthy infection.

Results

Failure of local MCs to degranulate and rapidly recruit neutrophils following *S.* Typhimurium infection

MCs possess an apparent inability to evoke protective responses in mice following *S.* Typhimurium infection. To address this failure, we hypothesized that *S.* Typhimurium is able to inactivate MCs. In order to test this notion, we injected late log phase *S.* Typhimurium SL1433 into the peritoneal cavity of WT and MC-deficient $Kit^{W\text{-}sh}/Kit^{W\text{-}sh}$ (MC-deficient) mice. We chose the peritoneum for the following reasons: (i) it is a self-contained body site where bacterial numbers and neutrophil influx can be simultaneously and conveniently assessed, (ii) bacteria can directly interact with MCs, and (iii) MCs can be readily visualized in the peritoneal fluid in order to determine activation status by evaluating cell morphology. Interestingly, we observed no significant difference in the bacterial burdens of peritoneal lavage from WT and MC-deficient mice upon infection with *S.* Typhimurium (Figure 1A, top). Consistent with this finding, myeloperoxidase (MPO) assays of lavage revealed no significant difference in neutrophil influx between the two groups of mice (Figure 1A, bottom). In contrast, when *E. coli* J96 was intraperitoneally injected into the two mouse strains, a significant difference in bacterial clearance was observed between WT and MC-deficient mice (Figure 1B, top). This observation correlated with an increased neutrophil influx in WT mice compared to MC-deficient mice (Figure 1B, bottom). The lack of an appreciable difference in bacterial load between WT and MC-deficient mice is consistent with previous reports that found no clear protective function for MCs during *S.* Typhimurium infection (Piliponsky et al., 2010). To determine whether our observations could be related to differential MC activation upon contact with different pathogens, we investigated the morphology of MCs in the peritoneal fluid (Figure 1C, top) and mesentery (bottom) of both groups of mice. For comparative purposes, we also examined MCs from PBS-injected mice. MCs from mice challenged with *E. coli* J96 were not readily visible by toluidine blue staining, as they were extensively degranulated with an observable spray of isolated granules around each MC (Figure 1C, middle). In contrast, MCs from *S.* Typhimurium-challenged mice were readily detectable and fully granulated (Figure 1C, right) and morphologically resembled MCs from controls (Figure 1C, left). Quantification of fully & partially granulated MCs at both of these sites is provided in Figure 1D. These observations collectively suggest that, unlike their vigorous response to *E. coli* J96, MCs appear incapable of evoking a degranulation response to *S.* Typhimurium. Consequently, limited neutrophil responses and corresponding bacterial clearance were observed in *S.* Typhimuriuminfected mice.

S. Typhimurium actively suppresses degranulation of murine and human MCs

To more closely investigate the limited MC degranulation response to *S.* Typhimurium, we utilized the MC model cell line RBL-2H3 in standard *in vitro* β-hexosaminidase release assays to assess MC degranulation activity following exposure to *S.* Typhimurium, *E. coli* J96, or ionomycin, a potent MC secretagogue which works by triggering intracellular calcium flux (Gilfillan and Tkaczyk, 2006). Whereas ionomycin and *E. coli* J96 evoked significant responses, no degranulation was observed in response to *S.* Typhimurium or to PBS (Figure 2A). Compared to dose-dependent MC degranulation observed with *E. coli* J96

(Figure 2B, left), the degranulation response to *S.* Typhimurium was minimal (Figure 2B, right).

The limited MC degranulation to *S.* Typhimurium could potentially be attributable to the ability of *S.* Typhimurium to actively block MC degranulation or to the inability of MCs to evoke a response to *S.* Typhimurium. To test the latter possibility, we exposed MCs to live and heat-killed *S.* Typhimurium and observed that MCs failed to degranulate to either stimulus, indicating that the MCs were inherently unresponsive to *S.* Typhimurium (Figure 2C, left). Next, to investigate whether *S.* Typhimurium also possesses the ability to inhibit MC degranulation, we pre-treated MCs with live or heat-killed *S.* Typhimurium and then exposed the cells to the potent secretagogue ionomycin. We found that in contrast to killed *S.* Typhimurium, live *S.* Typhimurium was able to block subsequent MC responses to ionomycin (Figure 2C, right), indicating that *S.* Typhimurium has the innate capacity to actively block the MC degranulation. To assess the specificity of this activity, we pre-treated MCs with live *E. coli* strain CI5 or the Gram-positive pathogen *Staphylococcus aureus* and found that neither of these bacteria were able to inhibit the MC degranulation to ionomycin (Figure 2D).

As these observations were made in a rodent cell line, we sought to confirm them in the LAD2 human MC cell line. Pre-treatment of human MCs with *S.* Typhimurium not only blocked subsequent responses to ionomycin but also to other known secretagogues, C48/80 and complement fragment C5a (Figure 2E). This suggests that *S.* Typhimurium possesses both the ability to circumvent MC activation and but also the capacity to suppress the MC degranulation response to activators utilizing distinct signaling pathways, suggesting a multipronged inhibitory activity.

SptP suppresses MC by dephosphorylating Syk and N-ethylmalemide-sensitive factor (NSF)

Virulence factors associated with *S.* Typhimurium are typically encoded by genes located in one or more pathogenicity islands. Therefore, we examined *S.* Typhimurium null mutants for the two best characterized pathogenicity islands, SPI1 and SPI2, as well as a double mutant (SPI1&SP2) for their ability to block MC degranulation. In contrast to the SPI2 mutant (Δ*SPI2*), we found that the SPI1 mutant (Δ*SPI1*) as well as the double SPI1&SPI2 mutant (Δ*SPI1&2*) failed to block ionomycin-induced degranulation (Figure 3A). The SPI1 T3SS translocates multiple effectors directly into host cells, many of which activate or impede specific cellular functions (Haraga et al., 2008). Since MC degranulation requires a tyrosine phosphorylation cascade (Gilfillan and Tkaczyk, 2006), we postulated that a possible MC suppressor was the Salmonella Protein Tyrosine Phosphatase (SptP), a known SPI1 effector with distinct phosphatase and GTPase activities (Kaniga et al., 1996).

To investigate the role of SptP in suppressing MC activity, we first compared the ability of WT *S.* Typhimurium and an isogenic mutant Δ*sptP* to prevent degranulation. Here, we used IgE+antigen as the MC stimulant because this well-characterized signaling pathway has several potential targets for phosphatase activity. We found that in the case of MCs pretreated with Δ*sptP* mutant, the degranulation response to IgE stimulation was no longer inhibited and was even higher than that seen with IgE stimulation (Figure 3B). One

possibility for the enhanced degranulation response of Δ*sptP* treated MCs is that the GTPase-activating protein (GAP) domain of SptP also has a known effect promoting recovery of cellular cytoskeleton after *Salmonella* mediated invasion (Fu and Galan, 1999). In the absence of reorganized cytoskeleton as is the case with Δ*sptP* mutant, MCs degranulate excessively following stimulation (Foger et al., 2011).

Next, we undertook a series of complementation studies to identify the relevant region in the functionally distinct domains located at either end of SptP. To distinguish the effects between the GTPase-activating function of the amino-terminal region and the protein tyrosine phosphatase function associated with the carboxy-terminal region (Fu and Galan, 1999; Kaniga et al., 1996), we complemented Δ*sptP S.* Typhimurium with the plasmid *psptP*^{WT} encoding WT *sptP*, *psptP*^{C481S} encoding *sptP* with an inactive phosphatase domain, or *psptP*^{R209A} encoding *sptP* with an inactive GTPase domain and compared the ability of the complemented strains to suppress MC degranulation (Figure 3B). Complementation with *psptP*^{WT} or with *psptP*^{R209A} but not with *psptP*^{C481S} inhibited MC degranulation in comparison to the Δ*sptP* mutant. These results suggest that SptP, and specifically the catalytic activity of its tyrosine phosphatase domain, mediates MC degranulation.

To investigate if SptP has the inherent ability to suppress MC degranulation, we cloned and expressed SptP intracellularly in the RBL-2H3 MC cell by stably transfecting with SptP-eGFP, resulting in SptP expression in approximately 60% of cells based on fluorescent activity (Figure S2). We next examined the effects of SptP expression on the MC degranulation response to IgE+anti-IgE in RBL-2H3 cells. We observed that RBL-2H3 MC cells transfected with S ptP-eGFP exhibited a significant (~60%) reduction in degranulation compared to the control (Figure 3C).

To facilitate trafficking of SptP into the MC cytosol via non-endocytic pathways after exogenous treatment of SptP, we constructed a membrane-permeant SptP by conjugating it to the short peptide RKKRRQRRR derived from the HIV TAT (transactivator of transcription) protein, which can translocate itself into the cytosol of various host cells (Gump and Dowdy, 2007). To observe SptP-TAT penetrance into bone marrow-derived mast cells (BMMCs), we employed confocal microscopy to visualize the protein within BMMCs. We opted to employ BMMCs here to make the point that observations made using the RBL-2H3 cell line were also applicable to primary MCs. We observed that SptP-TAT readily entered BMMCs and could even be detected in the nuclei (Figure 3D, bottom). Due to its superior ability to penetrate MC membranes, we predicted that SptP-TAT would effectively block the MC degranulation response. We observed that in contrast to controls, SptP-TAT significantly inhibited IgE+anti-IgE mediated degranulation in a dose-dependent manner (Figure 3E). We also generated a catalytically inactive form of SptP-TAT, SptP^{C481S}-TAT that had been observed in cytosol and nuclei (data not shown), to specifically ablate the tyrosine phosphatase activity. Unlike SptP-TAT, recombinant SptP^{C481S}-TAT was unable to inhibit IgE+anti-IgE-mediated BMMC degranulation (Figure 3F), confirming that SptP inhibits degranulation using its tyrosine phosphatase activity.

Next, we sought to localize sites of tyrosine phosphorylation in MCs during degranulation and determine their activation following exposure to SptP-TAT. Confocal microscopy of BMMCs employing probes for MC granules and phosphotyrosine revealed that tyrosine phosphorylation appeared to be localized primarily to empty compartments where granules were housed prior to activation with IgE+anti-IgE (Figure 3G, middle, arrowheads). This is consistent with the notion that not only is tyrosine kinase activity important in the signaling events leading to degranulation, but it is also important in the final stages of granule release (Mustelin et al., 2005). We thus hypothesized that intracellular SptP could interfere with the regulation of the granule secretory pathway to block MC degranulation. In SptP-TAT treated BMMCs (Figure 3G, right), which did not degranulate following exposure to IgE+anti-IgE, no tyrosine phosphorylation was observed in the granule chambers, which is consistent with a lack of degranulation. Notably, detectable amounts of SptP were localized to the granule compartments. Thus, the absence of tyrosine phosphorylation proximal to sites of granule discharge contributes to abrogated MC degranulation in SptP-TAT-treated MCs.

The SptP-TAT-associated absence of tyrosine phosphorylation in MCs led us to seek putative SptP targets in the IgE signaling pathway. Syk, a tyrosine kinase, is an important substrate in IgE-mediated MC degranulation (Gilfillan and Tkaczyk, 2006; Masuda and Schmitz, 2008), and thus we examined the effects of SptP on Syk activation following IgE mediated activation. SptP overexpression in transfected MCs markedly suppressed the Syk phosphorylation following stimulation with IgE+anti-IgE (Figure 3H, top). To further confirm the role of Syk, we also compared IgE-mediated Syk phosphorylation in MCs pre-treated with WT or Δ*sptP S.* Typhimurium. Consistent with SptP overexpression, WT *S.* Typhimurium markedly suppressed Syk phosphorylation, whereas Δ*sptP S.* Typhimurium failed to do so. Indeed, Δ*sptP S.* Typhimurium appeared to enhance Syk phosphorylation, indicating that in the absence of SptP, *Salmonella* might directly activate MCs and that the signaling events involve Syk (Figure 3H, bottom).

We also noticed that although granules of RBL-2H3 cells were not released following 1 h exposure WT *S.* Typhimurium, they appeared to have fused with each other resulting in abnormally large intracellular granules (Figure 3I, middle). However, this phenotype was not observed in MCs exposed to Δ*sptP S.* Typhimurium (Figure 3I, right). A critical determinant of MC degranulation is NSF, a vesicle fusion protein localized to the cytoplasmic side of granule membrane (Benhamou and Blank, 2010; Mustelin et al., 2005). In the steady state, NSF is typically phosphorylated which is important for keeping MC granules from spontaneous intracellular fusion (Huynh et al., 2004). Upon MC activation, NSF became dephosphorylated promoting fusion of granule membranes to plasma membranes resulting in extracellular release of MC granules. We suspected that in WT *S.* Typhimurium infected MCs, NSF is prematurely dephosphorylated, resulting in granule fusion without extracellular release. To validate this notion, control-treated, WT, and Δ*sptP S.* Typhimurium infected MCs were stained for NSF. In all cases, NSF colocalized to the outer surface of MC granules (Figure 3I). Furthermore, the granules of WT *S.* Typhimurium infected MCs appeared 2–3 times the size of regular granules of control MCs and Δ*sptP S.* Typhimurium infected MCs, suggesting intergranular fusion in the former (Figure 3I). To determine if intergranular fusion was associated with dephosphorylation of NSF, we

examined phosphorylation of NSF around MC granules and found that whereas NSF appeared phosphorylated around MC granules of PBS or Δ*sptP S.* Typhimurium treated MCs, this was not the case in WT *S.* Typhiumrium treated MCs (Figure 3J, middle). Furthermore, when we immunoprecipitated NSF from the three groups of MCs and probed with anti-phosphotyrosine antibodies on a western blot, we observed that in contrast to the other two conditions, NSF in WT *S.* Typhimurium infected MCs was markedly dephosphorylated (Figure 3K) providing support to our notions of premature intergranular fusion induced by *S.* Typhimurium phosphatases. That SptP acts at sites downstream of Syk can also be inferred by the fact that WT *S.* Typhimurium, but not Δ*sptP* and Δ*sptP(psptP*^{C481S}*)* blocks ionomycin induced degranulation (Figure S1), which acts downstream of receptor mediated MC signaling events (Gilfillan and Tkaczyk, 2006).

A homologous tyrosine phosphatase produced by *Yersinia pestis* blocks MC degranulation

We have noted that SptP shares appreciable homology with phosphatases naturally found in MCs to prevent excessive activation (Kaniga et al., 1996; Wang et al., 2002) (data not shown). *Yersinia pestis* is another Gram-negative pathogen that expresses a potent tyrosine phosphatase, YopH, which shares marked structural homology with SptP (Kaniga et al., 1996; Stebbins, 2004). Importantly, this enzyme is also injected into host cells via T3SS (Cornelis, 2002). In view of the similarities in terms of structure and delivery of these phosphatases, we speculated that MC suppression may be an evolved virulence trait shared among sophisticated pathogens such as *S.* Typhimurium and *Yersinia* and hypothesized that YopH could also suppress MC degranulation. We exposed MCs to a WT laboratory strain of *Yersinia pestis* KIM5 and examined the subsequent ability of these MCs to mount degranulation to ionomycin. *Y. pestis*-exposed MCs exhibited a significantly inhibited degranulation (Figure 4A). To determine whether YopH was the specific *Yersinia* factor involved in MC suppression, we cloned and expressed this tyrosine phosphatase in RBL-2H3 cells. In contrast to control eGFP-transfected cells, MCs transfected with YopH-eGFP had limited degranulation to IgE+antigen (Figure 4B). Figure 4C demonstrates the intracellular expression of YopH, granulation status of treated MCs, and tyrosine phophorylation of eGFP- and YopH-eGFP-transfected RBL-2H3 cells following exposure to IgE+antigen. In particular, MC degranulation seemed directly correlated with tyrosine phosphorylation in empty granule chambers (Figure 4C, middle, arrow heads) of IgE +antigen activated control MCs but not in YopH expressing MCs (Figure 4C). Next, we cloned and expressed YopH as a fusion protein with TAT. To determine whether exogenous YopH-TAT would inhibit MC degranulation, we exposed IgE-sensitized MCs to increasing concentrations of YopH-TAT and examined their responses to antigen-induced activation. We observed a significant and dose-dependent suppression of the MC degranulation response to antigen (Figure 4D). Taken together, these observations indicate that YopH shares the ability of SptP to suppress degranulation and suggest that MC suppression may be an important virulence trait among host-adapted pathogens.

Δ*sptP S.* Typhimurium induces MC degranulation, neutrophil influx and bacterial clearance

To investigate the *in vivo* contribution of SptP to MC suppression during *S.* Typhimurium infection, we challenged the peritoneal cavities of mice with WT or Δ*sptP S.* Typhimurium

(Figure 5A) and determined that MCs isolated from the peritoneal cavities exhibited widely different phenotypes in terms of their granulation status. MCs exposed to WT *S.* Typhimurium remained fully granulated (Figure 5A, third column), but MCs exposed to Δ*sptP S.* Typhimurium underwent extensive degranulation (Figure 5A, fourth column). This degranulation in response to the Δ*sptP* mutant when quantitated was comparable to the degranulation observed with *E. coli* J96 (Figure 5B), which was included for comparative purposes. The vacant granule chambers in extensively degranulated MCs stained strongly for tyrosine phosphorylation (Figure 5A, fourth column, arrowhead), whereas granule chambers in MCs exposed to *S.* Typhimurium or PBS failed to exhibit tyrosine phosphorylation staining. We observed that the overall phosphotyrosine fluorescence in Δ*sptP*-infected MCs was markedly higher (Figure 5A, fourth column) than *E. coli*-infected MCs. This enhanced tyrosine phosphorylation was previously observed in Δ*sptP*-exposed MCs *in vitro* (data not shown), which also consistently exhibited higher Syk phosphorylation than IgE+anti-IgE positive control cells (Figure 3H, bottom). This is potentially due to the fact that significantly higher degranulation was observed with Δ*sptP S.* Typhimurium than with the positive degranulation control (Figure 3B). As MC degranulation has been closely associated with neutrophil recruitment and subsequent bacterial clearance, we compared neutrophil responses in the peritoneum of mice following 4 h challenge with WT or Δ*sptP S.* Typhimurium. Predictably, we observed significantly higher neutrophil responses with Δ*sptP* than with WT *S.* Typhimurium (Figure 5C), and this correlated with greater clearance of Δ*sptP* compared to WT *S.* Typhimurium 24 h after bacterial challenge (Figure 5D), which were recovered by complemented mutant strain (Δ*sptP(psptP*^{WT}*)*) (Figure S3).

S. Typhimurium utilizes SptP to inhibit MC-dependent neutrophil influx and bacterial clearance

Given the intrinsic ability of SptP to block MC degranulation, previous studies have not been able to demonstrate a specific role for MCs in combating *S.* Typhimurium infections in WT and MC-deficient mice. Indeed, when we initially compared neutrophil responses and bacterial clearance in WT and MC-deficient mice following intraperitoneal challenge with WT *S.* Typhimurium, we failed to notice any appreciable difference between the two strains of mice (Figure 1A, 1C). However, based on our subsequent findings, we sought to demonstrate a potential MC response to *S.* Typhimurium by employing our Δ*sptP* mutant strain. We compared neutrophil responses and bacterial clearance of Δ*sptP S.* Typhimurium in WT and MC-deficient mice following peritoneal challenge. Neutrophil responses to Δ*sptP S.* Typhimurium was significantly more elevated in WT mice compared to MC-deficient mice (Figure 6A, top), and this was accompanied by better clearance of Δ*sptP S.* Typhimurium in WT mice 24 h after bacterial challenge (Figure 6A, bottom).

To demonstrate the potency of the MC suppressing activity of SptP-TAT, we co-administered recombinant SptP-TAT i.p. with *E. coli* J96, which normally activates MCs, and examined neutrophil recruitment and bacterial clearance. Compared to *E. coli* J96 alone, *E. coli* J96 co-instilled with SptP-TAT evoked lower neutrophil responses, and bacterial clearance from the peritoneum. To verify that this weak neutrophil response was linked to MCs, we examined isolated peritoneal MCs and found that those from mice challenged with

E. coli J96 with SptP-TAT were undegranulated (Figure 6C, right column) in contrast to mice challenged with *E. coli* J96 alone (Figure 6C, middle column, quantitated in Figure 6D). Furthermore, these undegranulated MCs exhibited a limited degree of tyrosine phosphorylation and appeared to have accrued detectable amounts of SptP-TAT in granule compartments (Figure 6C, right column).

MC-mediated neutrophil recruitment is also associated with vascular leakage of serum components, including complement and antibodies, that can markedly impact pathogen persistence in tissue sites (Kunder et al., 2011; Nakamura et al., 2009). We sought to examine the impact of SptP on MC-mediated vascular leakage by assessing the tissue penetrance of intravenously administered FITC-dextran. Figure 6E shows the whole mount staining of mouse ears that were intradermally injected with vehicle or SptP-TAT followed by *E. coli* J96 infection. Based on the large amount of FITC-dextran in the perivascular space (Figure 6E, middle), *E. coli* J96-injected tissue exhibited a high degree of vascular leakage. A high degree of MC degranulation was also observed in this tissue. In contrast, no vascular leakage and MC degranulation was observed in tissue injected with *E. coli* and S ptP-TAT (Figure 6E, right). A significant reduction in vascular leakage induced by SptP-TAT following *E. coli* J96 infection was quantitatively measured by examining extravasated Evans Blue in mouse ears (Figure S4). Additional whole mount staining revealed that SptP-TAT inhibited degranulation following exposure to *E. coli* J96 (Figure S5) and that this inhibitor could be detected in the cytosol of MCs in infected tissue (Figure S6). Cumulatively, these findings demonstrate that SptP is a potent suppressor of MC-mediated activity, and in the absence of SptP, MCs would likely play an antibacterial role during infection with *S.* Typhimurium.

MC-*S.* Typhimurium interactions likely occur immediately after the gut epithelium is breached

During natural infection, *S.* Typhimurium that successfully breach the gut epithelial barrier typically target the mesenteric lymph nodes, where they proliferate with limited interference from the host immune system (Mastroeni et al., 2009). However, before *S.* Typhimurium can reach the draining lymph nodes, the bacteria must circumvent an array of MCs present in the lamina propria of the gut epithelium. Shown in Figure S7 are sections of the caecal epithelium of mice challenged with PBS, WT *S.* Typhimurium or Δ*sptP S.* Typhimurium. Numerous fully granulated MCs were seen proximal to the epithelium in PBS or WT *S.* Typhimurium challenged mice but not in mice challenged with Δ*sptP S.* Typhimurium which are incapable of suppressing MCs. Indeed, the apparent absence of fully granulated MCs in the caecum of Δ*sptP S.* Typhimurium challenged mice was attributable to extensive MCs degranulation induced by the many mutant *S.* Typhimurium found at this site (Figure S7). We investigated whether these MCs in the lamina propria played a role in controlling bacterial numbers, thus suggesting a plausible role for *S.* Typhimurium-mediated MC suppression during natural infection. To address this question, we assessed the number of bacteria that reached the mesenteric lymph nodes in WT and MC-deficient mice shortly after oral challenge with Δ*sptP S.* Typhimurium, which does not suppress MCs. If gut-resident MCs contribute to bacterial clearance, we would expect fewer bacteria to reach the mesenteric nodes in MC-sufficient mice compared to their MC-deficient counterparts. W e

detected markedly greater numbers of bacteria in the immediate draining lymph nodes of MC-deficient mice 24 h after oral infection with Δ*sptP S.* Typhimurium compared to WT mice (Figure 7A). Because some recent studies have questioned the use of *Kit* dependent MC deficient mice (Benhamou and Blank, 2010; St John and Abraham, 2013; Urb and Sheppard, 2012), we have also included here a recently described *Kit* independent inducible model of MC deficiency, involving *Cma1-cre*$^{+}$*iDTR*$^{+}$ mice (Benhamou and Blank, 2010). Using this model, we obtained very similar findings regarding the contribution of MCs in the clearance of Δ*sptP S.* Typhimurium (Figure 7B). Additionally, we confirmed the contribution of the phosphatase domain of SptP by challenging WT and MC-deficient mice with Δ*sptP(psptP*^{C481S}*) S.* Typhimurium (Figure 7C). To confirm that the SptP deletion was responsible for MC-dependent bacterial clearance, we also infected WT and MC-deficient mice with Δ*sptP(psptP*^{WT}*) S.* Typhimurium (Figure 7D). Predictably, we observed that the bacterial burden in MC-sufficient mice was now comparable to that of MC-deficient mice. This result is also consistent with the data presented in Figure 1A demonstrating that the WT S. Typhimurium burden was comparable in MC-sufficient and MC-deficient mice. Thus, MCs have the potential to regulate the colonization of the mesenteric lymph nodes, which are among the first sites targeted by pathogens that successfully breach the gut barrier.

Discussion

In this study, we have revealed a highly effective mechanism employed by *S.* Typhimurium to elude host innate immunity involving the inactivation of MCs, immune surveillance cells strategically located at host-environment interfaces. We demonstrated that unlike *E. coli* J96, which provoked rapid and extensive MC degranulation, *S.* Typhimurium not only failed to elicit the MC degranulation response but also prevented MC responses to a wide array of potent secretagogues such as IgE+antigen, calcium ionophore and complement revealing a broad and powerful inhibitory activity (Figure 2, 3B). This capacity to block MC responses to other signals is relevant during infection because even though *S.* Typhimurium do not activate MCs *per se*, various endogenous danger signals or alarmins are released at infection sites which can potentially activate MCs (Pushparaj et al., 2009). *In vivo* studies in mice revealed that this innate capacity of *S.* Typhimurium to block MC degranulation markedly reduced neutrophil responses and limited bacterial clearance at the infection site. This is in sharp contrast to *E. coli*, which elicited extensive MC degranulation, a strong neutrophil response, and marked bacterial clearance from the site of infection. This capacity to elude early innate immune responses by inactivating peripheral MCs may explain, at least in part, the well-recognized ability of *S.* Typhimurium to avoid clearance by the innate immune system and to disseminate rapidly from the site of infection to distal sites such as the draining lymph nodes and liver (Mastroeni et al., 2009). Our observation that *S.* Typhimurium inhibited early neutrophil recruitment is not inconsistent with earlier reports of strong neutrophil responses following *S.* Typhimurium infection (Cheminay et al., 2004; Yang et al., 2002). In this study, we focused on a narrow window of time during the early stages of the infection process, but observed the development of a vigorous MC-independent neutrophil response at sites of infection with WT *S.* Typhimurium after the initial lag period (data not shown). Our findings imply that the initial immune response to a pathogen is an important determinant of infection outcome. A delayed neutrophil response at the site of *S.*

Typhimurium infection, regardless of it s intensity, may have limited protective value because many of the bacteria are either intracellular or have become systemic at that point.

The ability of *S.* Typhimurium to block MC activity could, at least in part, explain why others have not been able to demonstrate a protective role for MCs (Chatterjea et al., 2005). Much of our conclusions were based using traditional *Kit* mutant MC deficient mice, however, since this model of MC deficiency has been challenged recently (Benhamou and Blank, 2010; St John and Abraham, 2013; Urb and Sheppard, 2012), we sought to confirm our findings employing *Kit* independent *Cma1-cre*$^{+}$*iDTR*$^{+}$ mice where the MC deficiency was inducible. Our findings utilizing the inducible model of MC deficiency corroborated findings with *Kit* mutant mice providing further validation of our conclusions.

S. Typhimurium mediated suppression of MC degranulation was achieved through introduction of SptP into the MC cytosol. The suppressing actions of SptP are restricted to the exocytic function of MCs because MCs readily internalize *S.* Typhimurium upon contact. SptP is a SPI1 effector protein with two functional domains. The N-terminal domain functions during pathogen entry into host cells by deactivating Rho GTPases and reversing pathogen-induced cytoskeletal changes following *S.* Typhimurium uptake (Fu and Galan, 1999). The second, C-terminal domain comprises a protein tyrosine phosphatase reported to function late in the pathogen entry process when *S.* Typhimurium is harbored within late endosomes (Humphreys et al., 2009). In these compartments, it is believed that SptP dephosphorylates a protein that facilitates cellular membrane fusion and protein degradation, enhancing intracellular *S.* Typhimurium replication. The tyrosine phosphatase domain of SptP is also thought to inactivate MAP kinase (Murli et al., 2001). Our finding that the tyrosine phosphatase region of SptP mediates MC inactivation represents a distinct function for this domain, while our work with GTPase-inactive SptP as well as YopH, which lacks a GTPase domain, suggests that GTPase activity is for the most part dispensable for MC suppression. A comparison of the primary structure of SptP with multiple tyrosine phosphatases found in the cytosol of MCs reveals high degree of homology (Kaniga et al., 1996), implying multiple targets for this phosphatase. Morphological studies of MCs employing pTyr-specific antibody probes revealed that degranulation was closely associated with phosphorylation events at the cell surface as well as at intracellular sites proximal to cytosolic granules. Phosphorylation of these proteins at both sites did not occur in the presence of SptP, suggesting that SptP acted at multiple sites and on multiple targets. By examining *S.* Typhimurium infected MCs before or after activation with various secretagogues we have been able to identify at least two distinct substrates for SptP. Immunoblot analyses of *S.* Typhimurium-infected MCs and control MCs following IgE mediated activation revealed one of the intracellular targets of SptP to be Syk, which is a member of the Syk/Zap-70 family, and a substrate found early in the signaling cascade. Microscopic and immunoprecipation studies of MCs infected with WT *S.* Typhimurium also revealed that shortly after infection MC granules spontaneously coalesced forming oversized granules which failed to be expelled upon subsequent exposure to potent secretegogues. This phenomenon was not observed with Δ*sptP S.* Typhimurium indicating that it was an SptP mediated activity. We have linked this intergranular fusion to SptP mediated

dephophorylation of NSF, a fusion protein whose functions include preventing homotypic intergranular fusion (Mustelin et al., 2005; Wang et al., 2002).

Although a number MC-inactivating compounds derived from various microbes have been identified, including the toxic fungal metabolite gliotoxin (Cramer et al., 2006; Niide et al., 2006), ES-62, a glycoprotein secreted by filarial nematodes (Melendez et al., 2007), FK506 from *Streptomyces tsukubaensis* (Narenjkar et al., 2006), and cyclosporine A from *Tolypocladium inflatum* (Harrison et al., 2007), these do not, for the most part, appear to be relevant in the pathogenesis of infection. Our studies here reveal that two highly successful host-adapted pathogens, *S.* Typhimurium and *Y. pestis*, share a powerful mechanism to suppress MC degranulation, suggesting that MC inhibition is an important virulence determinant. MCs are one of the first immune cells encountered by these pathogens after they traverse the epithelial barrier. They are relatively abundant in dermal tissue, where *Y. pestis* is localized following injection by fleas, and also common in the gut epithelium below Peyer's patches as well as in the lamia propria, where they can encounter *S.* Typhimurium invading through M cells or gut epithelial cells (Jones et al., 1994). Orally-administered *S.* Typhimurium that successfully breach the epithelial barrier traffic to the mesenteric lymph nodes, a process likely to be influenced by MC interactions. Indeed, significantly higher numbers of the Δ*sptP* mutant were present in the mesenteric nodes of MC-deficient mice following oral infection, implicating mucosal MCs as primary responders to *S.* Typhimurium breaching the gut epithelium.

MCs and MC-like cells are found in a wide range of animal species including less evolved species devoid of an adaptive immunity. In recent years it has become clear that MCs play a key role in modulating innate immune responses to various bacteria, parasites, viruses and fungi suggesting that the *raison d'être* for these cells is modulation of immediate and nonspecific immunity to microbial challenge. In view of this it is not surprising that certain virulent pathogens would have evolved special mechanisms to inactivate these cells to prevent or delay host immune responses and promote their pathogenesis.

Experimental Procedures

Bacterial strains and culture

S. Typhimurium SL1344, SL1344-derived Tn5 transposon insertion mutants in *SPI1*, *SPI2*, and *SPI1&2* were gifts from Dr. Alejandro Aballay, Duke University. SB300, and its *sptP* deletion mutant, SB749, were gifts from Dr. Jorge E. Galán, Yale University. Δ*sptP(psptP*^{WT}*)*, Δ*sptP(psptP*^{C481S}*)*, and Δ*sptP(psptP*^{R209A}*)* were generated in this study. Other strains used include *E. coli* J96 and CI5, a Gram-positive clinical isolate *Staphylococcus aureus* strain 54 (Duke University Medical Center), and a WT laboratory strain of conditionally virulent and naturally occurring *Yersinia pestis* KIM5. Bacteria were grown for 15 h, non-shaking, in Luria-Bertani (LB) (Gibco) broth at 37°C. 25 μg/ml kanamycin was added for transposon mutants, 100 μg/ml streptomycin for SB300 and SB749, and 100 μg/ml carbenicillin for complemented strains.

Mice

C57BL/6 mice were purchased from the National Cancer Institute. MC-deficient Wsh mice (*Kit*$^{W\text{-}sh}$/*Kit*$^{W\text{-}sh}$) and their congenic littermate controls were from Jackson Laboratories. To induce MC depletion, eight-week-old *Cma1-cre*$^{+}$*iDTR*$^{+}$ (a gift from Dr. Axel Roers, University of Technology, Dresden) and wild-type littermates received five i.v. injections of 100 ng DT per mouse in a week. All experiments were performed according to protocols approved by the Duke Division of Laboratory Animal Resources and the Duke University Institutional Animal Care and Use Committee.

Animal infections and CFU counts

Mice were infected i.p. with *S.* Typhimurium, or *E. coli* J96 in 100 μl sterile PBS. At indicated times, peritoneal lavage was performed with 5 ml sterile, ice-cold PBS. Lavage was analyzed for MC degranulation, neutrophil influx or CFU. Oral infection was as described (Barthel et al., 2003). Briefly, mice were pretreated with 20 mg streptomycin prior to infection with 5×10^7 CFU of Δ*sptP* or its complemented mutant *S.* Typhimurium. At various times, mice were sacrificed and mesenteric lymph nodes homogenized in 0.1% Triton X-100 per PBS. Lysates were plated on MacConkey agar with or without 50 μg/ml streptomycin and incubated overnight at 37°C for CFU.

Enzymatic assays

β-hexosaminidase assay and myeloperoxidase assay are described in the supplemental experimental procedures.

Microscopy

Staining of cultured BMMCs, peritoneal cells, the mesentery and ear tissue are described in the supplemental experimental procedures. A Nikon ECLIPSE TE200 microscope was used to obtain confocal images using a channel-series approach.

Statistical analysis

Results were analyzed with one-way ANOVA and Tukey's post-test or two-way ANOVA or the Mann-Whitney t-test as appropriate with Prism (GraphPad) software. Differences between groups were considered significant at $p<0.05$. All error bars represent SEM.

Supplementary Material

Refer to Web version on PubMed Central for supplementary material.

Acknowledgments

We thank J. Galán and A. Aballay for *Salmonella* strains; S. Dowdy for plasmids; D. Metcalfe for LAD2 cells; A. Roers for *Cma1-cre*$^{+}$*iDTR*$^{+}$ mice. We thank M. Kuehn, L. Hale and M. Gunn for discussions. C. Shelburne provided technical advice. W. Ang and S. Bowen provided critical manuscript review. This work was funded by US National Institutes of Health grants: U01-AI082107; R01-AI096305; R56- DK095198.

References

Abraham SN, St John AL. Mast cell-orchestrated immunity to pathogens. Nat Rev Immunol. 2010; 10:440–452. [PubMed: 20498670]

Barthel M, Hapfelmeier S, Quintanilla-Martinez L, Kremer M, Rohde M, Hogardt M, Pfeffer K, Russmann H, Hardt WD. Pretreatment of mice with streptomycin provides a Salmonella enterica serovar Typhimurium colitis model that allows analysis of both pathogen and host. Infection and immunity. 2003; 71:2839–2858. [PubMed: 12704158]

Benhamou M, Blank U. Stimulus-secretion coupling by high-affinity IgE receptor: new developments. FEBS letters. 2010; 584:4941–4948. [PubMed: 20851120]

Chatterjea D, Burns-Guydish SM, Sciuto TE, Dvorak A, Contag CH, Galli SJ. Adoptive transfer of mast cells does not enhance the impaired survival of Kit(W)/Kit(W-v) mice in a model of low dose intraperitoneal infection with bioluminescent Salmonella typhimurium. Immunol Lett. 2005; 99:122–129. [PubMed: 15894120]

Cheminay C, Chakravortty D, Hensel M. Role of neutrophils in murine salmonellosis. Infection and immunity. 2004; 72:468–477. [PubMed: 14688128]

Cheminay C, Mohlenbrink A, Hensel M. Intracellular Salmonella inhibit antigen presentation by dendritic cells. Journal of immunology. 2005; 174:2892–2899.

Cornelis GR. Yersinia type III secretion: send in the effectors. J Cell Biol. 2002; 158:401–408. [PubMed: 12163464]

Cramer RA Jr, Gamcsik MP, Brooking RM, Najvar LK, Kirkpatrick WR, Patterson TF, Balibar CJ, Graybill JR, Perfect JR, Abraham SN, Steinbach WJ. Disruption of a nonribosomal peptide synthetase in Aspergillus fumigatus eliminates gliotoxin production. Eukaryot Cell. 2006; 5:972–980. [PubMed: 16757745]

Dawicki W, Marshall JS. New and emerging roles for mast cells in host defence. Curr Opin Immunol. 2007; 19:31–38. [PubMed: 17126541]

Foger N, Jenckel A, Orinska Z, Lee KH, Chan AC, Bulfone-Paus S. Differential regulation of mast cell degranulation versus cytokine secretion by the actin regulatory proteins Coronin1a and Coronin1b. The Journal of experimental medicine. 2011; 208:1777–1787. [PubMed: 21844203]

Fu Y, Galan JE. A salmonella protein antagonizes Rac-1 and Cdc42 to mediate host-cell recovery after bacterial invasion. Nature. 1999; 401:293–297. [PubMed: 10499590]

Galan JE. Salmonella interactions with host cells: type III secretion at work. Annu Rev Cell Dev Biol. 2001; 17:53–86. [PubMed: 11687484]

Gilfillan AM, Tkaczyk C. Integrated signalling pathways for mast-cell activation. Nat Rev Immunol. 2006; 6:218–230. [PubMed: 16470226]

Gump JM, Dowdy SF. TAT transduction: the molecular mechanism and therapeutic prospects. Trends Mol Med. 2007; 13:443–448. [PubMed: 17913584]

Gunn JS, Ernst RK, McCoy AJ, Miller SI. Constitutive mutations of the Salmonella enterica serovar Typhimurium transcriptional virulence regulator phoP. Infection and immunity. 2000; 68:3758–3762. [PubMed: 10816543]

Guo L, Lim KB, Gunn JS, Bainbridge B, Darveau RP, Hackett M, Miller SI. Regulation of lipid A modifications by Salmonella typhimurium virulence genes phoP-phoQ. Science. 1997; 276:250–253. [PubMed: 9092473]

Haraga A, Ohlson MB, Miller SI. Salmonellae interplay with host cells. Nat Rev Microbiol. 2008; 6:53–66. [PubMed: 18026123]

Harrison CA, Bastan R, Peirce MJ, Munday MR, Peachell PT. Role of calcineurin in the regulation of human lung mast cell and basophil function by cyclosporine and FK506. Br J Pharmacol. 2007; 150:509–518. [PubMed: 17200674]

Hornef MW, Wick MJ, Rhen M, Normark S. Bacterial strategies for overcoming host innate and adaptive immune responses. Nat Immunol. 2002; 3:1033–1040. [PubMed: 12407412]

Humphreys D, Hume PJ, Koronakis V. The Salmonella effector SptP dephosphorylates host AAA+ ATPase VCP to promote development of its intracellular replicative niche. Cell host & microbe. 2009; 5:225–233. [PubMed: 19286132]

Huynh H, Bottini N, Williams S, Cherepanov V, Musumeci L, Saito K, Bruckner S, Vachon E, Wang X, Kruger J, et al. Control of vesicle fusion by a tyrosine phosphatase. Nature cell biology. 2004; 6:831–839.

Jones BD, Ghori N, Falkow S. Salmonella typhimurium initiates murine infection by penetrating and destroying the specialized epithelial M cells of the Peyer's patches. J Exp Med. 1994; 180:15–23. [PubMed: 8006579]

Kaniga K, Uralil J, Bliska JB, Galan JE. A secreted protein tyrosine phosphatase with modular effector domains in the bacterial pathogen Salmonella typhimurium. Mol Microbiol. 1996; 21:633–641. [PubMed: 8866485]

Kunder CA, St John AL, Abraham SN. Mast cell modulation of the vascular and lymphatic endothelium. Blood. 2011; 118:5383–5393. [PubMed: 21908429]

Malaviya R, Ikeda T, Ross E, Abraham SN. Mast cell modulation of neutrophil influx and bacterial clearance at sites of infection through TNF-alpha. Nature. 1996; 381:77–80. [PubMed: 8609993]

Marshall JS. Mast-cell responses to pathogens. Nat Rev Immunol. 2004; 4:787–799. [PubMed: 15459670]

Mastroeni P, Grant A, Restif O, Maskell D. A dynamic view of the spread and intracellular distribution of Salmonella enterica. Nature reviews. Microbiology. 2009; 7:73–80.

Masuda ES, Schmitz J. Syk inhibitors as treatment for allergic rhinitis. Pulm Pharmacol Ther. 2008; 21:461–467. [PubMed: 17669674]

McLaughlin LM, Govoni GR, Gerke C, Gopinath S, Peng K, Laidlaw G, Chien YH, Jeong HW, Li Z, Brown MD, et al. The Salmonella SPI2 effector SseI mediates long-term systemic infection by modulating host cell migration. PLoS pathogens. 2009; 5:e1000671. [PubMed: 19956712]

Mead PS, Slutsker L, Dietz V, McCaig LF, Bresee JS, Shapiro C, Griffin PM, Tauxe RV. Food21 related illness and death in the United States. Emerg Infect Dis. 1999; 5:607–625. [PubMed: 10511517]

Melendez AJ, Harnett MM, Pushparaj PN, Wong WS, Tay HK, McSharry CP, Harnett W. Inhibition of Fc epsilon RI-mediated mast cell responses by ES-62, a product of parasitic filarial nematodes. Nat Med. 2007; 13:1375–1381. [PubMed: 17952092]

Murli S, Watson RO, Galan JE. Role of tyrosine kinases and the tyrosine phosphatase SptP in the interaction of Salmonella with host cells. Cellular microbiology. 2001; 3:795–810. [PubMed: 11736992]

Mustelin T, Vang T, Bottini N. Protein tyrosine phosphatases and the immune response. Nat Rev Immunol. 2005; 5:43–57. [PubMed: 15630428]

Nakamura Y, Kambe N, Saito M, Nishikomori R, Kim YG, Murakami M, Nunez G, Matsue H. Mast cells mediate neutrophil recruitment and vascular leakage through the NLRP3 inflammasome in histamine-independent urticaria. The Journal of experimental medicine. 2009; 206:1037–1046. [PubMed: 19364881]

Narenjkar J, Assem el SK, Wan BY, Marsh S, Ezeamuzie CI. Effect of cyclosporin and tacrolimus (FK506) on the antigen-induced mediator release, membrane potential and 86Rb+/K+ and Ca2+ fluxes in the RBL-2H3 cell line. Int Immunopharmacol. 2006; 6:742–749. [PubMed: 16546704]

Niide O, Suzuki Y, Yoshimaru T, Inoue T, Takayama T, Ra C. Fungal metabolite gliotoxin blocks mast cell activation by a calcium- and superoxide-dependent mechanism: implications for immunosuppressive activities. Clin Immunol. 2006; 118:108–116. [PubMed: 16213796]

Piliponsky AM, Chen CC, Grimbaldeston MA, Burns-Guydish SM, Hardy J, Kalesnikoff J, Contag CH, Tsai M, Galli SJ. Mast cell-derived TNF can exacerbate mortality during severe bacterial infections in C57BL/6-KitW-sh/W-sh mice. Am J Pathol. 2010; 176:926–938. [PubMed: 20035049]

Pushparaj PN, Tay HK, H'Ng SC, Pitman N, Xu D, McKenzie A, Liew FY, Melendez AJ. The cytokine interleukin-33 mediates anaphylactic shock. Proceedings of the National Academy of Sciences of the United States of America. 2009; 106:9773–9778. [PubMed: 19506243]

Santos RL, Raffatellu M, Bevins CL, Adams LG, Tukel C, Tsolis RM, Baumler AJ. Life in the inflamed intestine, Salmonella style. Trends Microbiol. 2009; 17:498–506. [PubMed: 19819699]

St John AL, Abraham SN. Salmonella disrupts lymph node architecture by TLR4-mediated suppression of homeostatic chemokines. Nat Med. 2009; 15:1259–1265. [PubMed: 19855398]

St John AL, Abraham SN. Innate immunity and its regulation by mast cells. Journal of immunology. 2013; 190:4458–4463.

St John AL, Rathore AP, Yap H, Ng ML, Metcalfe DD, Vasudevan SG, Abraham SN. Immune surveillance by mast cells during dengue infection promotes natural killer (NK) and NKT-cell recruitment and viral clearance. Proc Natl Acad Sci U S A. 2011; 108:9190–9195. [PubMed: 21576486]

Stebbins CE. Structural insights into bacterial modulation of the host cytoskeleton. Curr Opin Struct Biol. 2004; 14:731–740. [PubMed: 15582397]

Suto H, Nakae S, Kakurai M, Sedgwick JD, Tsai M, Galli SJ. Mast cell-associated TNF promotes dendritic cell migration. Journal of immunology. 2006; 176:4102–4112.

Urb M, Sheppard DC. The role of mast cells in the defence against pathogens. PLoS pathogens. 2012; 8:e1002619. [PubMed: 22577358]

van der Velden AW, Copass MK, Starnbach MN. Salmonella inhibit T cell proliferation by a direct, contact-dependent immunosuppressive effect. Proc Natl Acad Sci U S A. 2005; 102:17769–17774. [PubMed: 16306269]

van der Velden AW, Dougherty JT, Starnbach MN. Down-modulation of TCR expression by Salmonella enterica serovar Typhimurium. Journal of immunology. 2008; 180:5569–5574.

Wang X, Huynh H, Gjorloff-Wingren A, Monosov E, Stridsberg M, Fukuda M, Mustelin T. Enlargement of secretory vesicles by protein tyrosine phosphatase PTP-MEG2 in rat basophilic leukemia mast cells and Jurkat T cells. Journal of immunology. 2002; 168:4612–4619.

Yang KK, Dorner BG, Merkel U, Ryffel B, Schutt C, Golenbock D, Freeman MW, Jack RS. Neutrophil influx in response to a peritoneal infection with Salmonella is delayed in lipopolysaccharide-binding protein or CD14-deficient mice. Journal of immunology. 2002; 169:4475–4480.

Highlights

- *Salmonella* Typhimurium specifically suppresses mast cell degranulation.
- Mast cell suppression reduced neutrophil influx early in *Salmonella* infection.
- SptP inhibited mast cell degranulation by dephosphorylating Syk and NSF.
- Compared to WT *Salmonella* the SptP mutant is cleared early in infection.

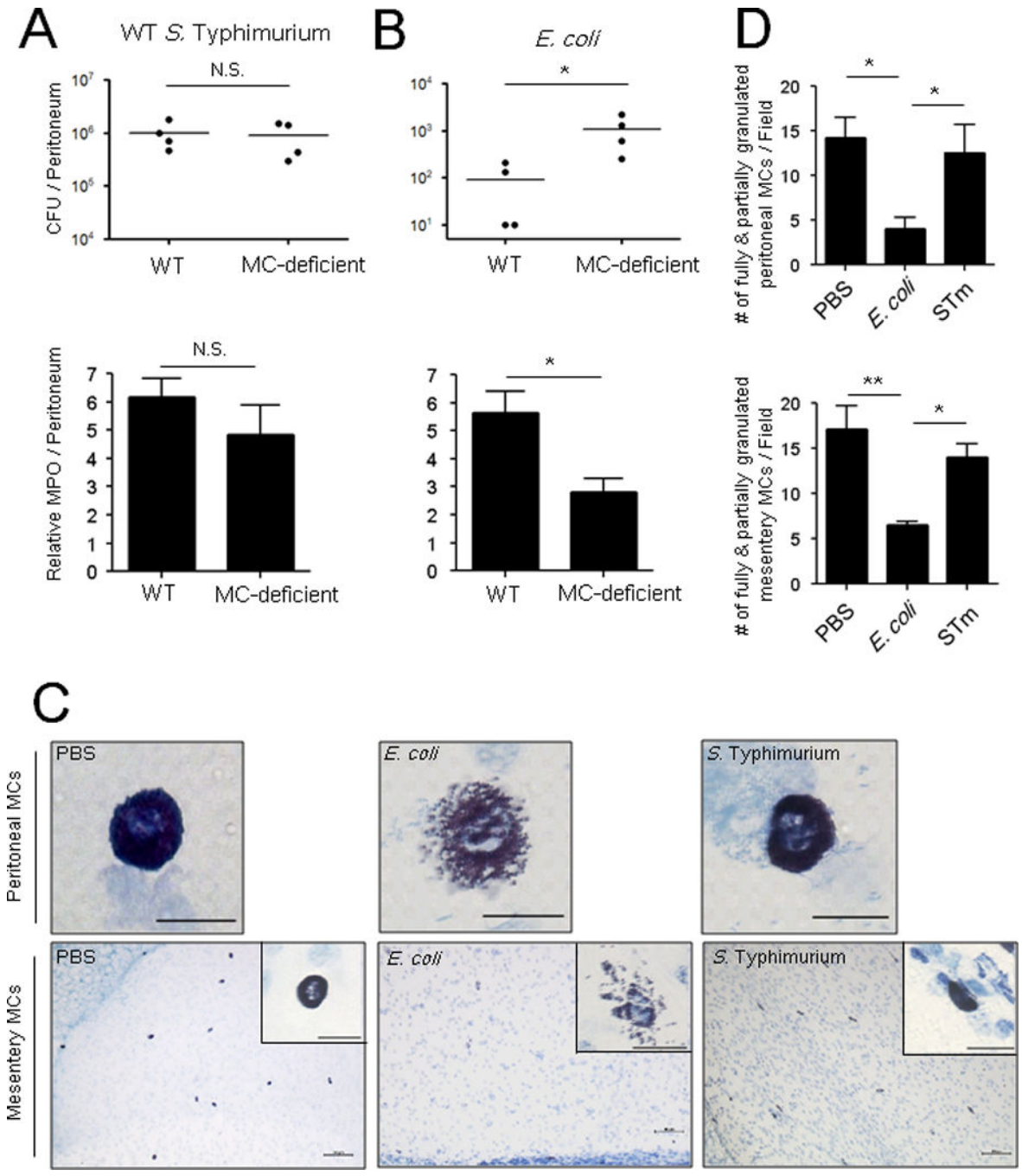

Fig 1. *S.* Typhimurium fails to elicit MC activation and subsequent neutrophil recruitment and bacterial clearance *in vivo*

(A, B, top) Residual bacterial counts (CFUs) in the peritoneal cavity of wild-type (WT) or MC-deficient mice 24 h following intraperitoneal (i.p.) infection with 5×10^5 CFU *S.* Typhimurium or 1×10^7 CFU *E. coli*. **(A, B, bottom)** Myeloperoxidase assay of peritoneal lavage of WT or MC-deficient mice 5 h post-infection with 1×10^7 CFU *S.* Typhimurium or *E. coli* J96 **(C)** Morphologic appearance of MCs in the peritoneum (top) and mesentery (bottom) of WT mice 3 h after i.p infection of 1×10^8 CFU *S.* Typhimurium or *E. coli* J96.

Insets represent 60X magnification of MCs in the mesentery. Images represent 3 independent experiments. Top panels and inset scale: 20 μm. Bottom panels scale: 100 μm. n=4. **(D)** Granulated MC numbers in peritoneal lavages (top) or mesentery whole mounts (bottom) were quantified by counting the number of partially and fully granulated MCs/field (n=3–5; 5 random chosen fields). Wholly degranulated MCs could not be detected. Mean ± SEM, *p<0.05, **P<0.01, N.S., not significant.

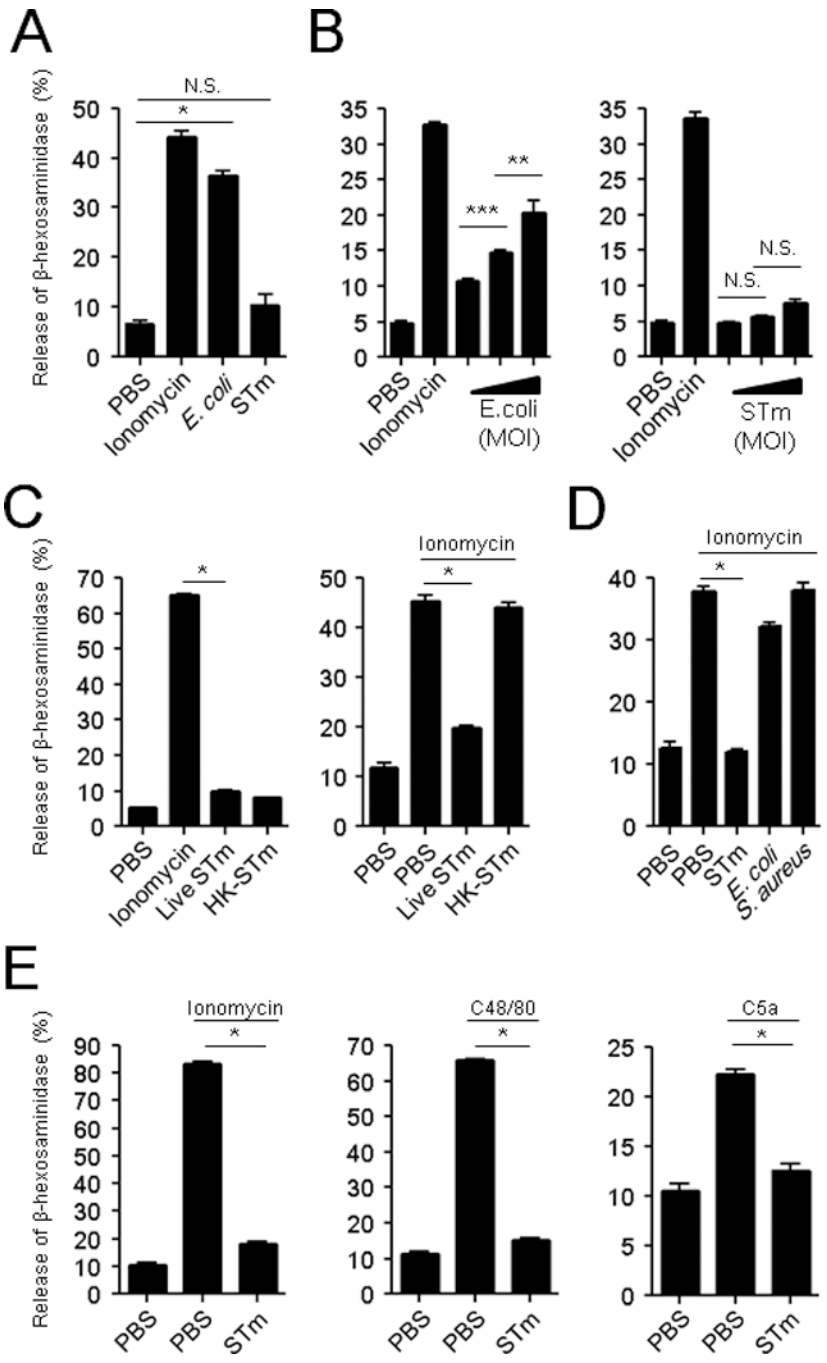

Fig 2. *S.* Typhimurium pretreatment actively suppresses MC degranulation to MC secretagogues

(A, B) *In vitro* β-hexosaminidase release assays of RBLs after 1 h exposure to *S.* Typhimurium (STm) or *E. coli* J96. **(B)** Effect of bacterial MOIs (10:1, 100:1, 1000:1) on MC degranulation. **(C, left)** β-hexosaminidase release by RBLs following 1 h exposure to live or heat-treated (60°C, 1 h) STm. **(C, right and D)** RBL degranulation to ionomycin after 30 min pretreatment with **(C, right)** live or heat-killed STm, and to **(D)** various bacteria. **(E)** LAD2 degranulation to ionomycin (left), C48/80 (middle), or C5a (right) after

30 min pretreatment with live STm or PBS (control). Mean ± SEM, *p<0.001, **p<0.01, ***p<0.05, N.S., not significant.

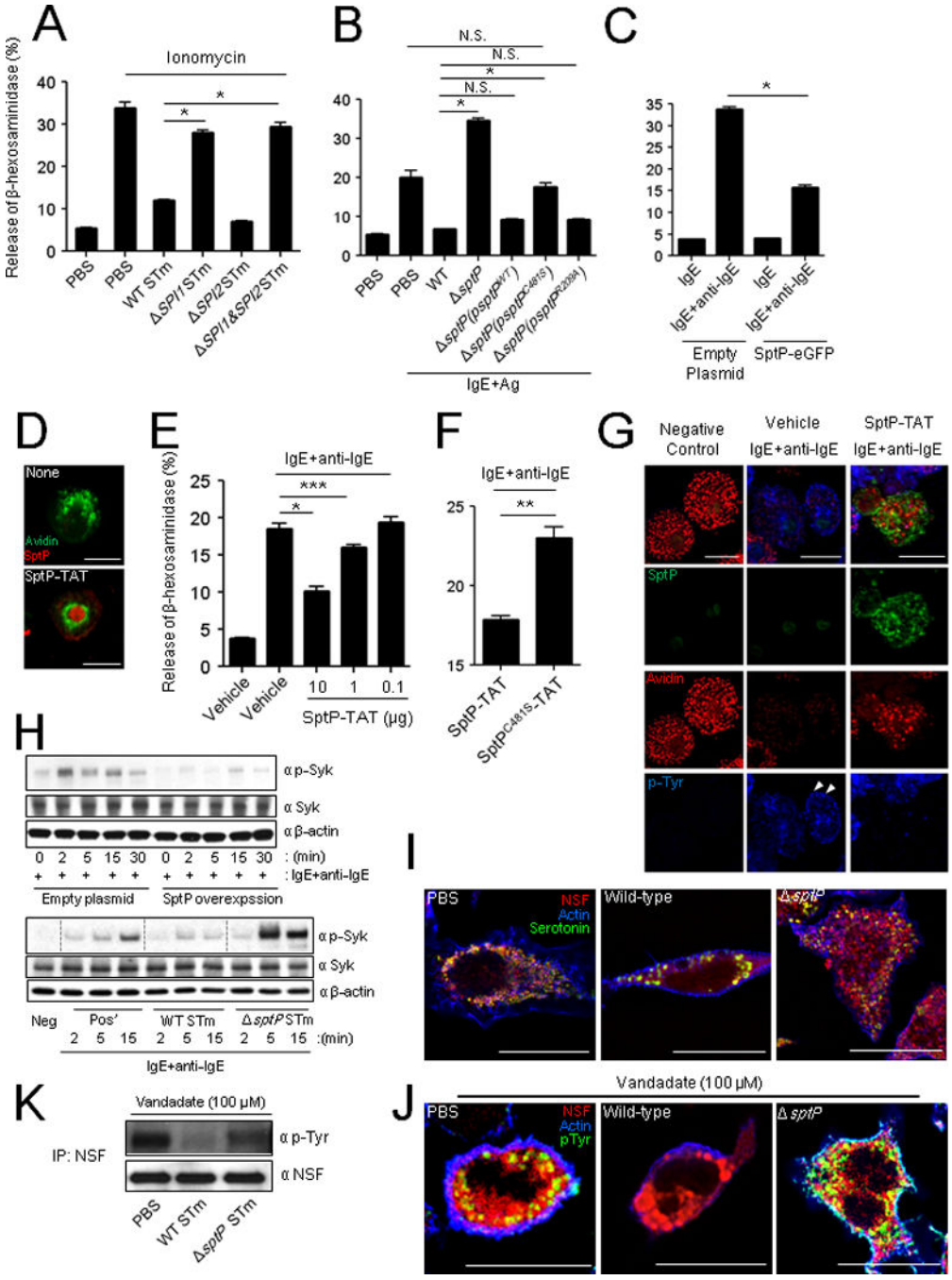

Fig 3. The protein tyrosine phosphatase domain of the SPI-1 effector, SptP, inhibits MC degranulation through dephosphorylating Syk and NSF

(A) MC degranulation to ionomycin after 30 min pretreatment with WT, Δ*SPI1* mutant, Δ*SPI2* or Δ*SPI1*&Δ*SPI2* STm strains **(B)** Degranulation of IgE sensitized MCs to antigen (Ag, TNP-OVA) after 45 min pretreatment with wild-type, Δ*sptP* or complemented Δ*sptP* strains (Δ*sptP*(*psptP*^{WT}), Δ*sptP*(*psptP*^{C481S}), or Δ*sptP*(*psptP*^{R209A})). **(C)** Degranulation of IgE sensitized MCs expressing retrovirally transduced eGFP or SptP-eGFP to anti-IgE. **(D)** Confocal microscopy of BMMCs exposed to SptP-TAT for 4 h. MC granules were probed

with avidin (green) and intracellular SptP-TAT probed with anti-His_6 (red). **(E and F)** Degranulation of IgE-sensitized BMMCs to anti-IgE **(E)** after 4 h pretreatment with increasing amounts of SptP-TAT (10, 1, and 0.1 μg) or **(F)** after 2 h pretreatment with SptP-TAT (5 μg) or $SptP^{C481S}$-TAT (5 μg). **(G)** Morphological appearance of IgE sensitized BMMCs to anti-IgE after 2 h pretreatment with vehicle or SptP-TAT (10 μg). MC granules: avidin (red), SptP-TAT: anti-His_6 (green), and intracellular tyrosine phosphorylation sites: anti-phosphotyrosine (p-Tyr) (blue) antibodies. **(H)** Western blots of cell preparations from IgE-sensitized RBLs that were either stably expressing SptP-eGFP or control eGFP (top) or were pretreated with WT STm or Δ*sptP* STm for 1 h (bottom) before activation with anti-IgE. The cell preparations from both experiments were obtained at indicated time points after activation with anti-IgE. Western blots were probed with α-p-Syk, α-Syk, and α-β-actin antibodies. **(I, J)** Morphology of RBLs after exposure to WT or Δ*sptP* STm. After 1 h treatment, **(I)** cells were stained with antibodies for fluorescence microscopy. MC granules: α-serotonin (green), NSF: α-NSF (red) antibodies and actin: phalloidin (blue). **(J, K)** After 1 h treatment, cells were treated with vanadate (100 μM) for 5 min to preserve tyrosine phosphorylation and **(J)** were stained with antibodies for fluorescence microscopy. NSF: α-NSF (red) and intracellular tyrosine phosphorylation: α-pTyr (green) and actin: phalloidin (blue). **(K)** Lysates from RBLs were analyzed by immunoprecipitation and immunoblotting for phosphotyrosine and NSF. Scale bar is 20 μm. Mean ± SEM, *$p<0.001$, **$p<0.01$, ***$p<0.05$. See also Figure S1 and S2.

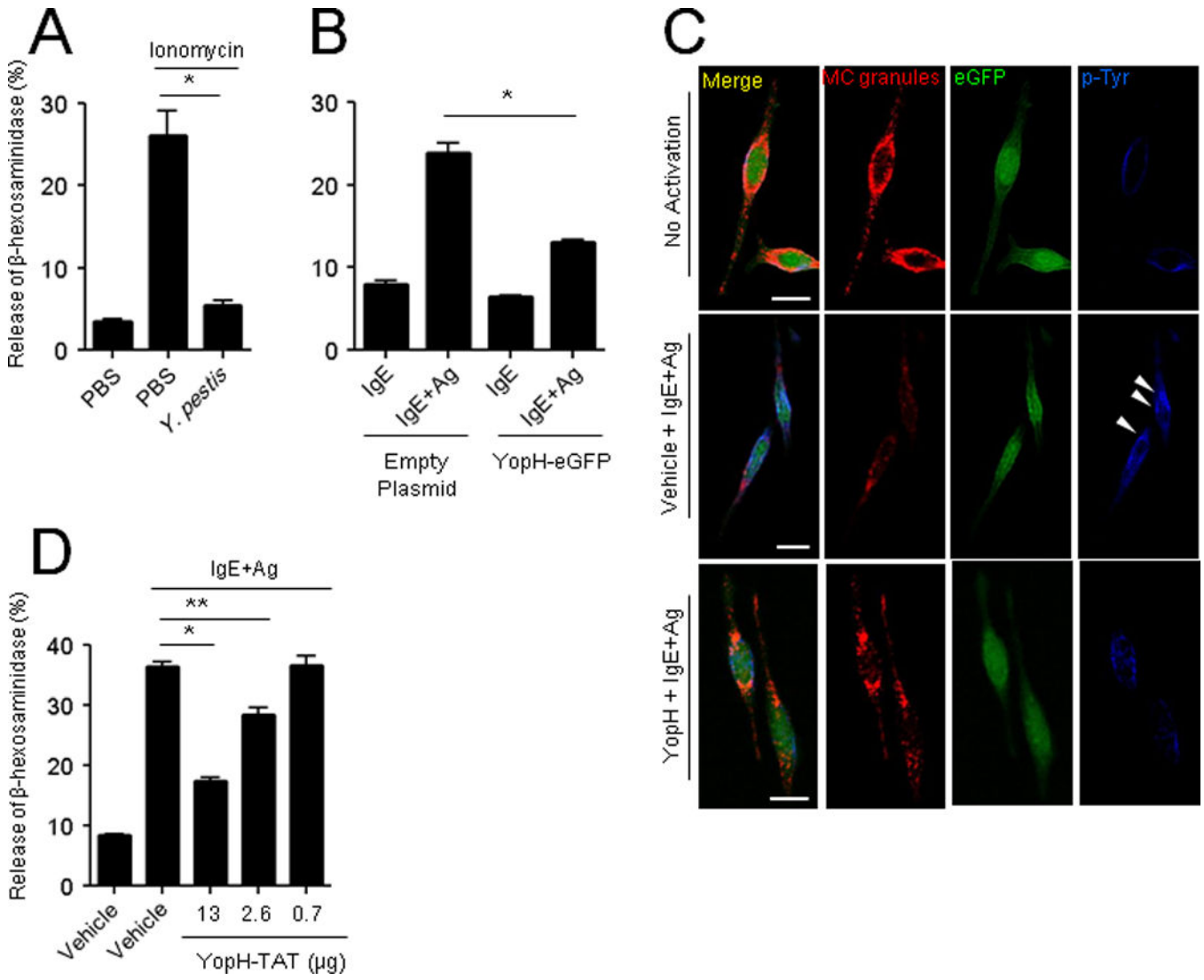

Fig 4. *Yersinia pestis* YopH suppresses MC activation

(A) Degranulation to ionomycin of RBLs pretreated for 30 min with PBS or *Y. pestis* KIM5. **(B and C)** RBLs were retrovirally transduced with control eGFP or YopH-eGFP before IgE +antigen stimulation (Ag, TNP-OVA) and assaying for degranulation **(B)**, or subjected to confocal microscopy **(C)**. Granules were stained with serotonin (red) and tyrosine phosphorylation with anti-p-Tyr antibody (blue). **(D)** Degranulation to IgE+Ag (TNP-OVA) RBLs following exposure to increasing concentration of purified YopH-TAT. Scale bar: 10 μm, mean ± SEM, *p<0.001, **p<0.01.

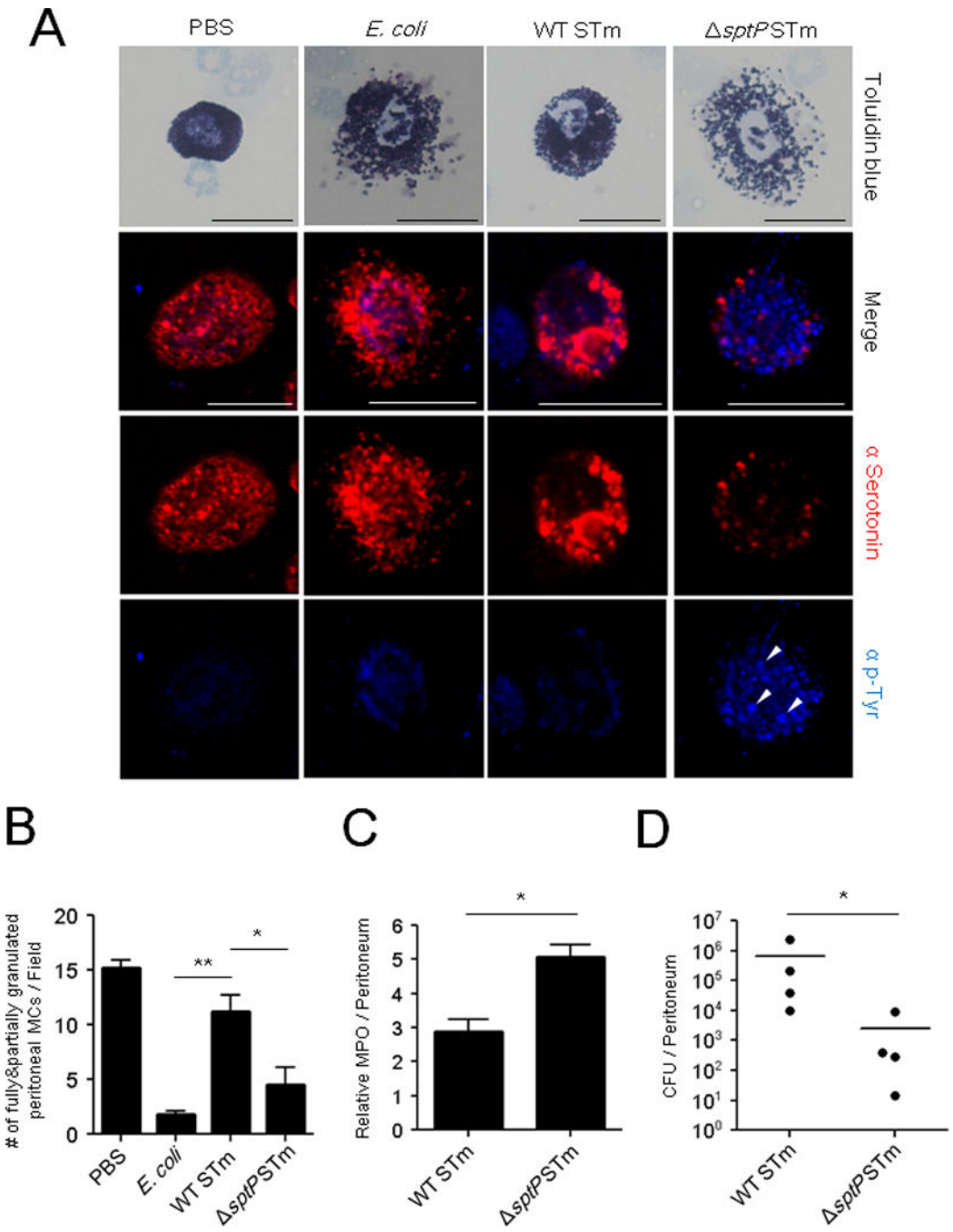

Fig 5. Infection of mice with Δ*sptP* activates MCs and enhances neutrophil recruitment and bacterial clearance compared to WT

(A) WT, Δ*sptP* STm, or *E. coli* J96. 1×10^8 CFU WT, Δ*sptP* STm, or *E. coli* J96 were injected i.p. Peritoneal lavage was harvested 4 h later, cytospun, and stained with toluidine blue for bright field microscopy (top) or with α-serotonin (red) for granules, and α-phosphotyrosine (blue) for immunofluorescence microscopy. **(B)** Granulated MC numbers in peritoneal lavages of (A) were quantified by counting partially and fully granulated MCs/field (n=3–6; 5 random chosen fields). Wholly degranulated MCs could not be detected. **(C)**

Assays for neutrophil recruitment (MPO) and **(D)** bacterial clearance (CFUs) were performed on lavages collected 4 h and 24 h, respectively, after i.p injection of 1×10^6 CFU WT or Δ*sptP* STm. n=4 mice, mean ± SEM, *p<0.05, **p<0.01. Scale bar: 20 μm. See also Figure S3.

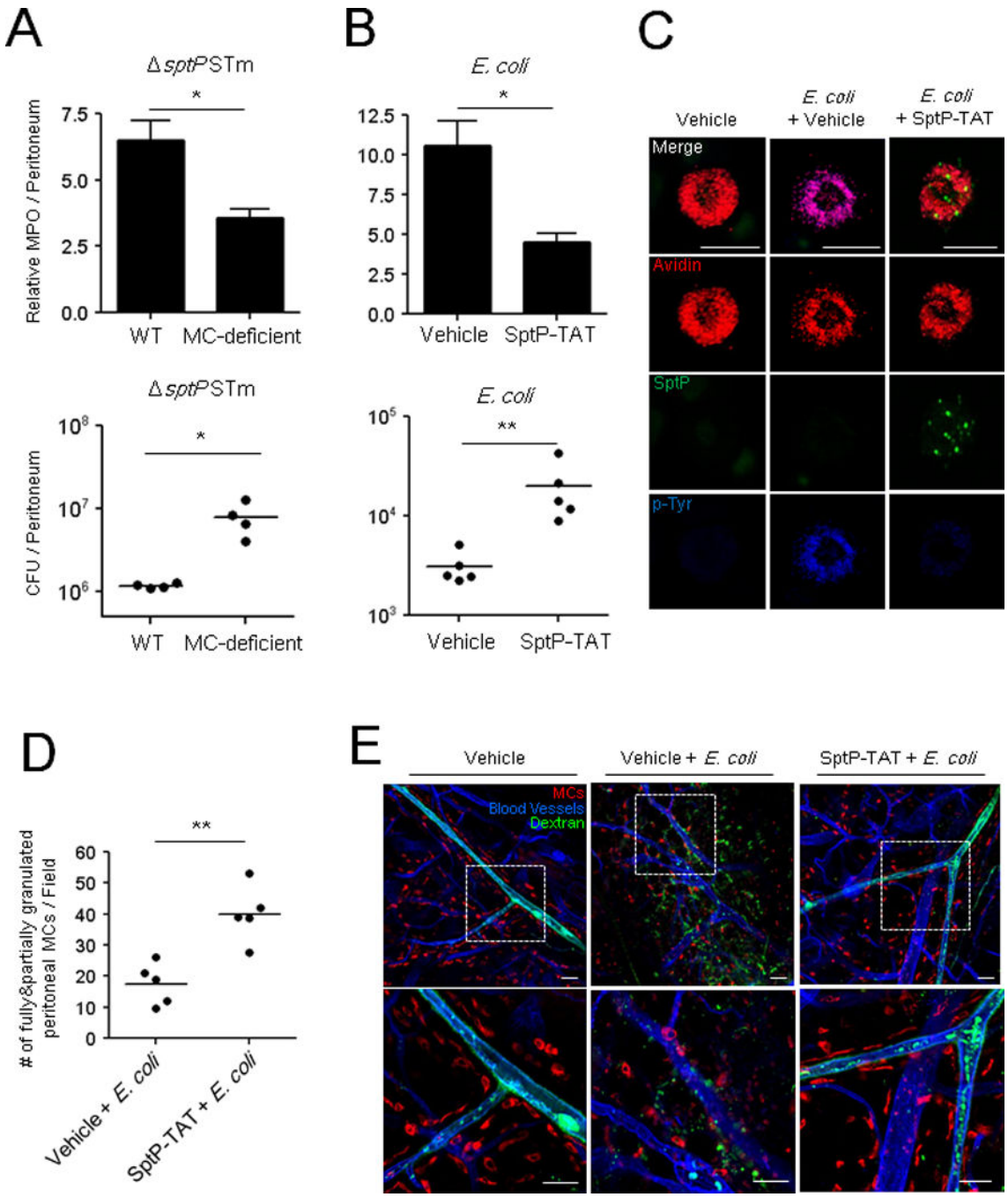

Fig 6. Δ*sptP S.* Typhimurium evokes MC-dependent neutrophil recruitment, bacterial clearance and vascular leakage

Neutrophil influx (top) and bacterial counts (bottom) in WT and MC-deficient mice **(A)** following i.p. injection of 5×10^5 CFU Δ*sptP* STm, **(B)** SptP-TAT (100 μg/mouse) or vehicle followed 30 min later with 1×10^7 CFU *E. coli.* MPO assays were performed 5 h post-infection and CFUs 24 h post-infection. (C) Morphology of MCs in the peritoneal cavities of control and SptP-TAT treated mice 3 h following *E. coli* infection. MC granules: avidin (red), SptP-TAT: anti-His_6 (green) and sites of tyrosine phosphorylation: anti-p-Tyr

antibodies (blue). Scale bars: 20 μm. **(D)** Granulated MC numbers in peritoneal lavages of **(C)** were quantified by counting the number of partially and fully granulated MCs/field (n=5; 5 random chosen fields). Totally degranulated MCs could not be detected. **(E)** Mouse ears were injected intradermally with vehicle or SptP-TAT (20 μg) and injected 1 h later with 1×10^6 CFU *E. coli* J96 at the same site and FITC-dextran (green) i.v.1 h post-infection, the ears were dissected, stained with avidin (red) and anti-CD31(blue), and whole mounted for immunofluorescence microscopy. Mean ± SEM, *p<0.05, **p<0.01. Scale bars: 50 μm. See also Figure S4, S5, and S6.

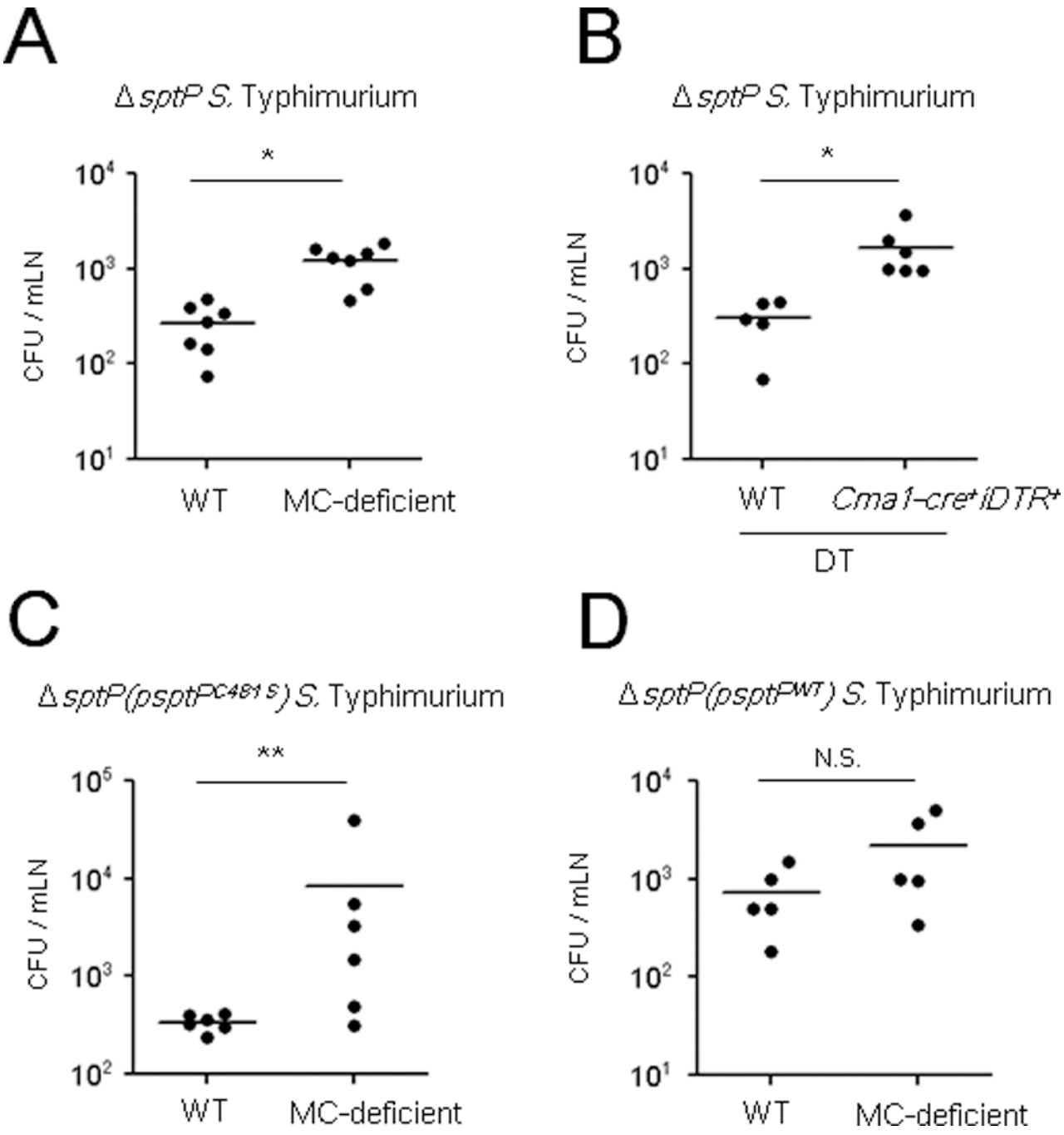

Fig 7. Intestinal MCs reduce bacterial burden in mesenteric lymph nodes following oral infection with Δ*sptP S.* Typhimurium

CFU of mesenteric lymph nodes in streptomycin-treated **(A, C, D)** WT or MC-deficient mice, **(B)** *Cma1-cre*$^{+}$*iDTR*$^{+}$ mice or WT controls after DT injections, following oral challenge with 5×10^{7} CFU **(A, B)** Δ*sptP S.* Typhimurium, **(C)** Δ*sptP(psptP*^{C481S}*)* and **(D)** Δ*sptP(psptP*^{WT}*)* 24 h post-infection. *p<0.01, **p<0.05, N.S., not significant. See also Figure S7.